Gas–Liquid Mass Transfer Intensification for Selective Alkyne Semi-Hydrogenation with an Advanced Elastic Catalytic Foam-Bed Reactor

Mohamad Fayad, Maïté Michaud, Han Peng, Vincent Ritleng, David Edouard

fluids

MDPI

Article

Gas–Liquid Mass Transfer Intensification for Selective Alkyne Semi-Hydrogenation with an Advanced Elastic Catalytic Foam-Bed Reactor

Mohamad Fayad [1], Maïté Michaud [1], Han Peng [2], Vincent Ritleng [2] and David Edouard [1,*]

[1] Catalyse Polymérisation Procédés & Matériaux, CP2M-UMR 5128 CNRS-CPE, Lyon UCBL, 43 Boulevard du 11 Novembre 1918, 69100 Villeurbanne, France
[2] Université de Strasbourg, Ecole Européenne de Chimie, Polymères et Matériaux, CNRS, LIMA, UMR 7042, 25 Rue Becquerel, 67087 Strasbourg, France
* Correspondence: david.edouard@univ-lyon1.fr

Abstract: The Elastic Catalytic Foam-bed Reactor (EcFR) technology was used to enhance a model catalytic hydrogenation reaction by improving gas–liquid mass transfer. This advanced technology is based on a column packed with a commercial elastomeric polyurethane open-cell foam, which also acts as a catalyst support. A simple and efficient crankshaft-inspired system applied in situ compression/relaxation movements to the foam bed. For the first time, the catalytic support parameters (i.e., porosity, tortuosity, characteristic length, etc.) underwent cyclic and controlled changes over time. These dynamic cycles have made it possible to intensify the transfer of gas to liquid at a constant energy level. The application chosen was the selective hydrogenation of phenylacetylene to styrene in an alcoholic solution using a palladium-based catalyst under hydrogen bubble conditions. The conversion observed with this EcFR at 1 Hz as cycle frequency was compared with that observed with a conventional Fixed Catalytic Foam-bed Reactor (FcFR).

Keywords: Elastic Foam-bed Reactor; open cell foam; mass transfer intensification; bubble reactor; polydopamine; hydrogenation; palladium; catalytic multiphasic reactor

Citation: Fayad, M.; Michaud, M.; Peng, H.; Ritleng, V.; Edouard, D. Gas–Liquid Mass Transfer Intensification for Selective Alkyne Semi-Hydrogenation with an Advanced Elastic Catalytic Foam-Bed Reactor. *Fluids* **2024**, *9*, 132. https://doi.org/10.3390/fluids9060132

Academic Editors: Kambiz Vafai and Stoyan Nedeltchev

Received: 29 January 2024
Revised: 22 May 2024
Accepted: 28 May 2024
Published: 1 June 2024

1. Introduction

Dissolution and mass transfer at the interface between gas and liquid phases is an important key for the design and optimization of many multiphase processes. Among the variety of multiphase systems, biological treatments of wastewaters, photo-bioreactors (e.g., microalgae production), and industrial applications (pharmaceutical products and catalytic reactions) all require an optimal gas (e.g., H_2, O_2, and CO_2,) dissolution and thus an intensification of mass transfer rate from the gaseous phase to the liquid phase.

For many reactors, the gas phase is often used in excess to overcome mass transfer limitations [1]. In fact, for industrial applications where flue gas (or industrial gaseous effluents) cannot be employed, the supply represents a significant operating cost and induces an eco-unfriendly process. Under these conditions and, generally, for multiphase catalytic reactors limited by mass transfer [2], process intensification is required [3,4]. As such, several reactor concepts and operation strategies have been proposed [4,5].

Structured catalytic supports including monoliths and open-cell foams can be used. In general, these structured supports provide high void space and specific surface area, together with a low-pressure drop [6,7]. In the open literature, many studies [8–13] also confirm the higher gas–liquid mass transfer coefficient (k_{la}) obtained with open-cell foams. With the advent of additive manufacturing, novel structured catalytic supports, including periodic open-cell structures, will allow the intensification of gas–liquid–solid contact [14,15].

Other techniques can be used in order to intensify gas–liquid processes. Periodic operation has been proposed [16,17]. For example, the liquid (and/or gas) flow rate is

supplied discontinuously and cyclically at the reactor inlet in order to induce a temporal modulation of the liquid holdup along the fixed bed to decrease the liquid film thickness surrounding the catalyst. Many lab-scale studies demonstrated a significant increase in k_{la} via flow modulation [18]. However, such induced liquid pulses rapidly decay along the fixed bed [19,20]. Moreover, the pressure drop can vary due to liquid pulses and have a negative impact on the global performance of the process. Härting et al. [21] introduced the inclined rotating fixed-bed reactor, where the reactor inclination and rotation allow a variation in the liquid holdup along the packed bed. After that, Dashliborun et al. [22] extended this intensification strategy for different systems; notably, for offshore CO_2 capture. However, with this technology, the reactor scale-up is rather difficult. More recently, Ferroni et al. [23] have designed an advanced potential catalyst support based on periodic open cellular structures. With this technology, it is possible to change the angle between the struts and the fluid direction at the inlet of the reactor. The characteristic change in position can be realized by a lifting or pilling motion at the beginning of the structure and consequently changes the gas-solid mass momentum transfer properties. This technology has not yet been tested for gas–liquid–solid systems and the problem of rapid decay along the fixed bed intensification remains with this technology. Even more complex techniques have been proposed in the open literature but are not, at this point, economically viable [4,24] (e.g., magnetic microgravity for multiphase catalytic rectors). In this context, it is necessary to develop new catalytic processes based on structured catalytic packing to improve the k_{la} with low energy consumption, especially in a low-flow interaction regime.

In this work, for the first time, the concept of an Elastic Catalytic-Foam-bed Reactor (EcFR) is presented and evaluated for a selective Pd-catalyzed alkyne semi-hydrogenation. In contrast to conventional fixed packing beds, the EFR (Elastic Foam-bed Reactor) technology, first introduced by Michaud et al. [25], uses a Soft Structured Catalytic Support [26–28], which allows the morphological properties of the internal bed to be modified in situ. Tortuosity, local porosity, local density, characteristic size of the medium, etc., are changed as a function of time. It is an innovative technological breakthrough in the field of gas–liquid systems.

For that purpose, we took advantage of the mechanical properties of a catalytic open-cell polyurethane foam (elastomeric polymer). The controlled compression/relaxation cycles were performed in the column under co-current up flow gas–liquid conditions. A simple and efficient crankshaft-inspired system was developed to control the EcFR process [25]. The performance (based on the reactant's conversion) with this EcFR shows that a kinetic regime is obtained in contrast to the FcFR (Fixed Catalytic Foam-bed Reactor) mode, which is limited by the overall volumetric gas–liquid mass transfer (k_{la}). These results show that, with a negligible increase in pressure drop, a possible intensification of the catalytic reaction can be achieved.

2. Materials and Methods

All reagents and solvents were used as provided by commercial suppliers without any further purification or treatment. Dopamine hydrochloride (008896) was purchased from Fluorochem (Paris, France). Tris base (99.9+%—T1503), styrene (99%), and $[PdCl_2(NH_3)_4]\cdot H_2O$ (≥99.9%—323438) were purchased from Sigma-Aldrich (Paris, France). Ethanol absolute (99%), phenylacetylene (99%), and ethylbenzene were purchased from Alfa Aesar (Paris, France). Gas chromatography (GC) analyses were conducted on a GC Agilent (Paris, France) with FID detectors using an HP-1 methyl siloxane column (10 m, 0.1 mm, 0.1 µm) with helium as the gas carrier and octane as the internal standard. Calibration curves were performed using pure phenylacetylene, styrene, and ethylbenzene at different concentrations after being diluted with ethanol. All conversions and selectivities were calculated using GC results.

High-resolution scanning electron microscopy (HR-SEM) analyses were carried out on a JEOL JSM-7900F SEM-FEG working at 2–7 kV accelerated voltage and at a distance of 6 to 10 mm. Images were obtained with a secondary electron detector. Samples were coated with a thin layer of carbon (ca. 10 nm) using a Balzer SCF004 (Paris, France) coater.

2.1. Elastic Foam Support

The elastic foam supports used in this work are commercially available polyurethane open-cell foams purchased from FoamPartner. The foam's characteristics (mechanical and morphological properties) are given in Table 1. Cylindrical samples (L_0 = 9 cm and ID = 32 mm) were used without prior treatment.

Table 1. Foam characteristics and effective parameters for typical operating conditions in this work (* estimated from SimFoam [29]).

Characteristic	Value
Strut size (d_s)	220 µm
Window size (a)	780 µm
Cell size (ϕ)	2500 µm
Density	0.027–0.033
Total porosity (ε)	0.97
Gas holdup (ε_g)	0.02 [13]
Liquid holdup (ε_l)	0.95 [13]
Specific surface area (a_c) *	1340 m^{-1}
Pressure drop *	15 Pa/m
Tortuosity *	1.24

2.2. Preparation of Catalytic Elastic Foam

According to the procedure described by Peng et al. [30], the following procedure was used in order to prepare the catalytic elastic foam.

- Coating of the polyurethane foam (PUF) with polydopamine (PDA)

A colorless aqueous solution of Tris base (10 mM), buffered to pH 8.5 with aqueous HCl (1M), was added to dopamine hydrochloride (2 mg/mL). A cylindrical sample of polyurethane foam (L_0 = 9 cm, ID = 3.2 cm) was then dipped in the stirred solution for 17 h at room temperature. The reaction medium turned rapidly orange, then progressively black. After this time, the resulting polydopamine-coated polyurethane foam (PDA@PUF) was removed from the medium, dried in an oven at 353 K for 90 min, then washed in water (3 × 10 min), and dried again in an oven at 353 K.

- Functionalization of PDA@PUF with $[PdCl_2(NH_3)_4]\cdot H_2O$

The prepared cylindrical sample of PDA@PUF was washed in stirred (725 rpm) H_2O/EtOH (1:5) for 1 h and dried under air before functionalization.

The PDA@PUF sample was then dipped in a stirred (725 rpm) solution of H_2O/EtOH (1:5) containing $[PdCl_2(NH_3)_4]\cdot H_2O$ (0.63 M). After 19 h, the resulting Pd-functionalized foam, Pd@PDA@PUF, was removed from the solution, washed in stirred water (3 × 10 min) and ethanol (2 × 10 min), dried in an oven at 353 K for 1 h, and characterized by high-resolution scanning electron microscopy (HR-SEM).

HR-SEM images of Pd@PDA@PUF are shown in Figure 1. The low magnification image (left) shows that polydopamine was coated on the whole surface of the foam as a rough film, while the higher magnification image (right) reveals that the rough film structure is constituted of dispersed polymer aggregates typical of polydopamine coating on a polyurethane foam [27,30]. No Pd particles could be identified, suggesting a relatively small size for the latter or, more likely, a molecular nature of the immobilized palladium species as the catechol moieties of the PDA layer may simply act as a chelating ligand [28,30].

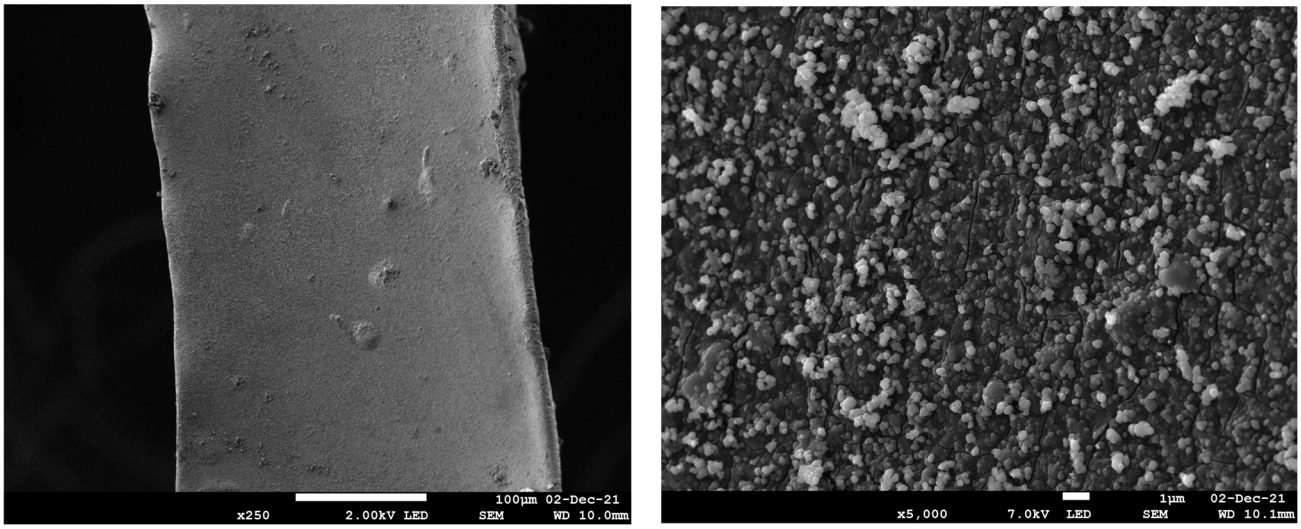

Figure 1. HR-SEM images with different magnifications of Pd@PDA@PUF.

ICP-AES measurements on several samples of Pd@PDA@PUF revealed a mean Pd loading of 2684 ± 93 mg/kg.

2.3. Reactor, Apparatus, and Phenylacetylene Semi-Hydrogenation Procedure

The schematic diagram of the experimental set-up used to investigate the FcFR and EcFR technologies is shown in Figure 2. The tubular reactor (ID = 32 mm (internal diameter), L = 0.25 m) was packed with two equal catalytic foam cylinders over a total bed height of 11 cm. The gas (dihydrogen—H_2) flow rate was controlled with a mass-flow controller (Brooks-Paris, France) and a peristatic pump (Stepdos 08S) was used to control the liquid flow. A static (not elastic) open-cell metal foam of 2 cm height was introduced at the entrance of the reactor in order to ensure uniform flow at the reactor inlet. A thermostatic bath (Lauda-Ultra 300) was used to maintain the reactor double jacket at a temperature of 323 K. A mini-motor (Mechatronic solutions—max 414 RPM-35 Watts) was used to rotate the mechanical wheel connected to a shaft (crankshaft) in order to move the perforated plate placed between the two catalytic foam cylinders inside the reactor (Figure 3). The movement of the perforated plate resulted in cyclic compression of one foam block while the other was relaxed and vice versa. Various technical problems had to be solved in this work, such as the possible leakage between the rod that ensures the movement of the perforated plate (via the crankshaft) and the bottom of the reactor. Also, it proved to be delicate to correctly attach the catalytic foam cylinders to the perforated plate.

During a typical experimental run, (i) the column was filled with a solution of phenylacetylene in ethanol, (ii) the power input by the heater was set to the desired value, (iii) the air trapped in the foam-bed was evacuated, and (iv) the flow rates were adjusted and the data recorded right after the H_2 gas was injected. For the FcFR mode, each catalytic foam was compressed to a fixed value of 40% (Figure 3). In contrast, in the case of the EcFR mode, each foam was compressed/relaxed as a function of time with a phase lag ($\varphi = \pi$) of 40% of the amplitude. In other words, the compression of each foam varied from 0 to 80% in this case. Thanks to the phase lag between the foam blocks one and two, the total contact time value ($tc = V/Q$) was constant for both configurations A and B (Figure 3). Consequently, under these conditions, it is then possible to compare the FcFR and EcFR technologies.

The monitored reaction was the selective semi-hydrogenation of phenylacetylene to styrene under H_2 (Figure 4). The reaction took place in an organic solvent, ethanol, at 323 K with Pd@PDA@PUF as the catalyst. Palladium catalysts have been widely used in the literature for the semi-hydrogenation of phenylacetylene in order to selectively produce styrene without the over-hydrogenation product ethylbenzene [30].

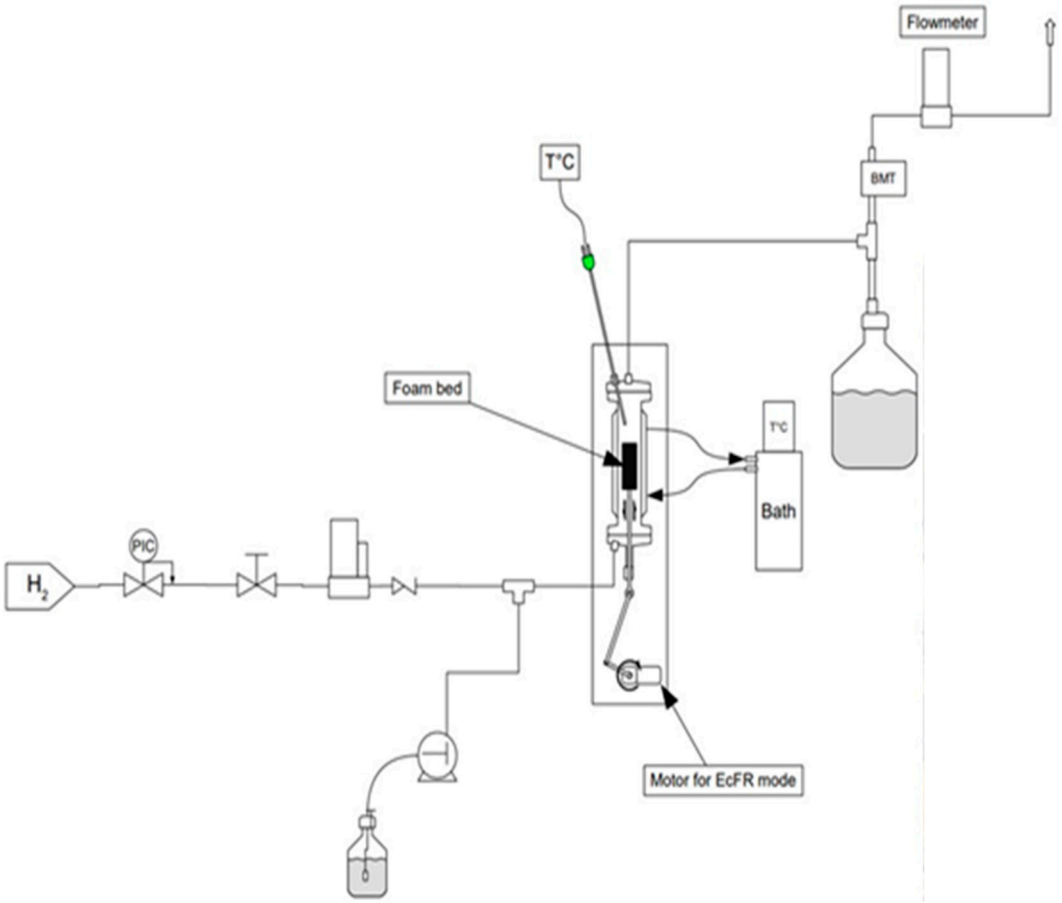

Figure 2. Schematic representation of the experimental setup and picture of the reactor.

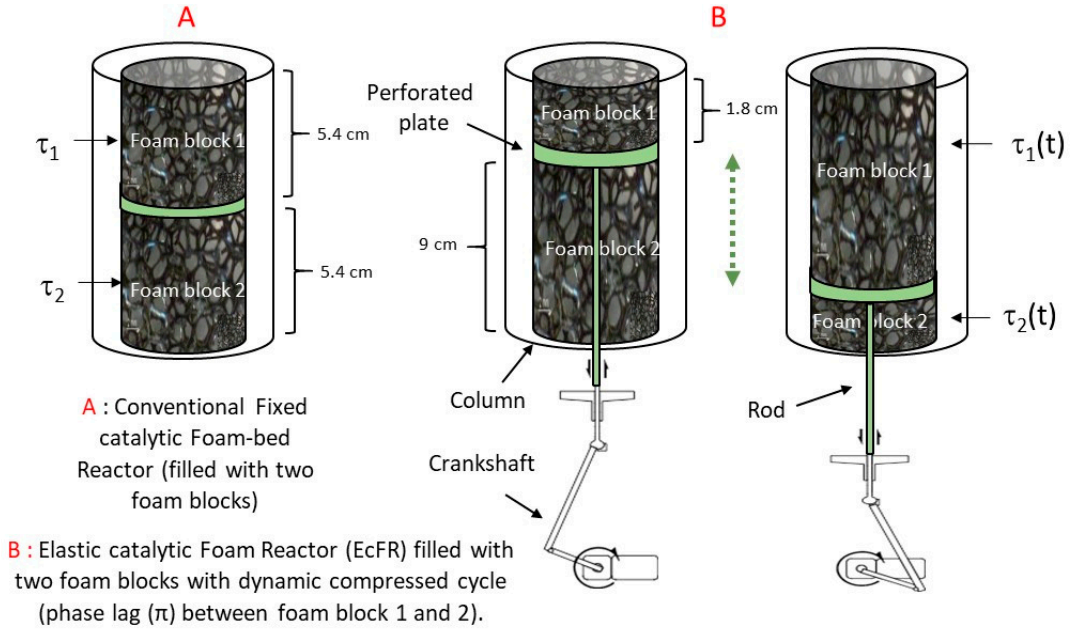

Figure 3. (**A**) FcFR mode: the catalytic foam blocks are compressed with a constant value of $\tau_1 = \tau_2 = 0.4$ (i.e., as in conventional fixed-bed foam packing). (**B**) EcFR mode: $\tau_1(t)$ and $\tau_2(t)$ varies between 0 and 0.8 with $\tau_1(t) = 0.4\sin(2\pi ft) + 0.4$ for foam block 1 and $\tau_2(t) = 0.4\sin(2\pi ft + \pi) + 0.4$ for foam block 2.

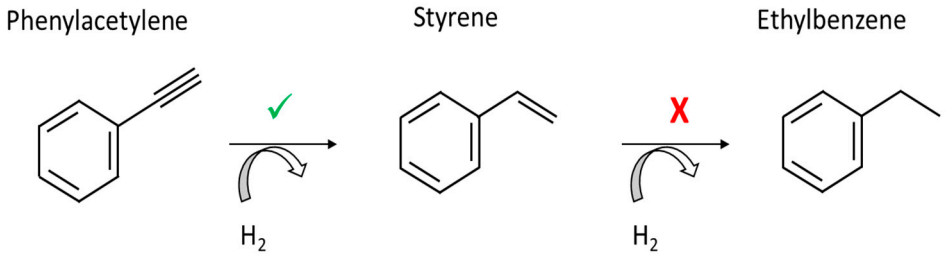

Figure 4. Selective phenylacetylene semi-hydrogenation.

For the reaction conversion monitoring at the reactor outlet, samples were taken in triplicate at given reaction times. The conversion, X, and reaction selectivity, S, were calculated according to the following equations:

$$X = \frac{C_{Ph0} - C_{Ph(t)}}{C_{Ph0}} \quad (1)$$

$$S = \frac{C_{S(t)}}{C_{S(t)} + C_{E(t)}} \quad (2)$$

with C_{Ph0} as the initial phenylacetylene concentration at the reactor inlet (kmol/m^3) and $C_{Ph(t)}$, $C_{S(t)}$, and $C_{E(t)}$ as the phenylacetylene, styrene, and ethylbenzene concentrations for a given sampling time, respectively.

3. Results

All experiments were conducted under atmospheric pressure and constant temperature (323 K), maintaining a constant inlet concentration of phenylacetylene (0.25 kmol/m^3), with octane serving as an internal standard at a concentration of 0.1 kmol/m^3 and ethanol as solvent. Two different liquid flow rates (2 mL/min and 5 mL/min) were tested for the selective hydrogenation of phenylacetylene with a constant hydrogen flow rate of 15 NmL/min.

It is noteworthy that before recording and analyzing the experimental data, more than 120 h of experiments were carried out with the Pd@PDA@PUF foams using the EcFR mode in order to remove all the fragile layers of polydopamine, resulting in an overall decrease in Pd loading on the foams. Hence, ICP-AES measurements on several samples of Pd@PDA@PUF revealed a mean Pd loading of 818 $\pm$ 24 mg/kg for the used foams, which contrasts with the mean Pd loading of 2684 $\pm$ 93 mg/kg measured for the as-synthesized foams.

Subsequently, in order to demonstrate that the concept of EFR could be studied with these catalytic foams, in other words, that no more palladium leaching occurred in the EcFR mode, and to show the stability and durability of the catalyst; a catalytic hydrogenation of phenylacetylene was carried out in the continuous mode for the FcFR and EcFR modes with a liquid flow rate of 5 mL/min for 800 min (Figure 5). Under the FcFR mode, a steady state of 19% conversion of phenylacetylene was reached after 100 min of reaction. Shifting the reactor mode from the FcFR mode to the EcFR mode led to an increase in conversion, reaching a value of 40%. Next, shifting the reactor mode back to FcFR mode led to a decrease in the conversion from 40% to 18%, as initially observed for the FcFR mode. These unambiguous results show that (i) thanks to the polydopamine properties, the concept of an Elastic Catalytic Foam-bed Reactor is possible (i.e., no palladium leaching occurred anymore) and that (ii) reaction intensification occurs in EcFR mode. It should be noted here that, in agreement with the literature results [30,31], the selectivity to styrene was 100% throughout all the experiment because the conversion is always less than 90%.

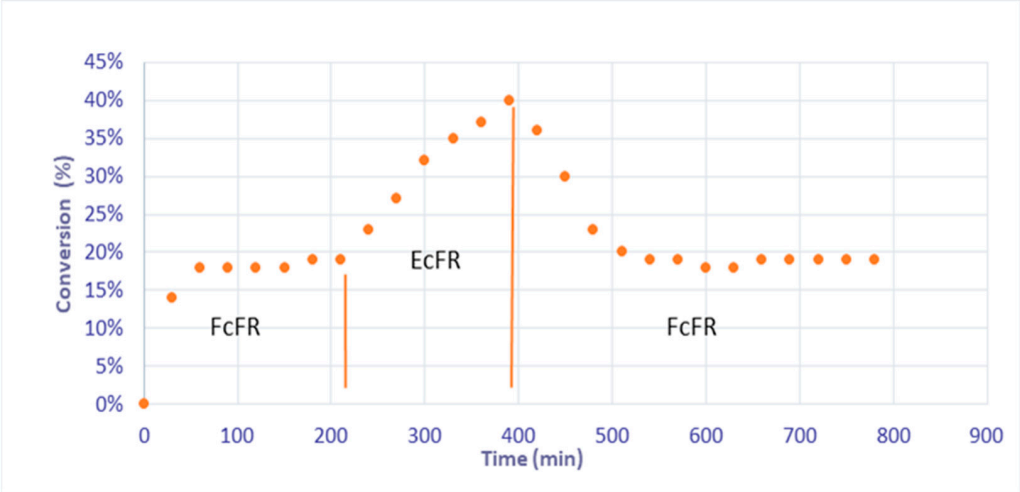

Figure 5. Conversion of phenylacetylene in FcFR/EcFR (f = 1 Hz) modes at a 5 mL/min liquid flow rate under continuous liquid and gas flows.

The selective hydrogenation of phenylacetylene was also studied at a flow rate of 2 mL/min. The conversion of phenylacetylene to styrene reached a value of 78% at the steady state after 550 min under the EcFR mode, while only a 44% value was reached using the FcFR mode (Figure 6a). These values are greater than those obtained for the EcFR and FcFR modes (45% and 19%) at a flow rate of 5 mL/min (Figure 6b)

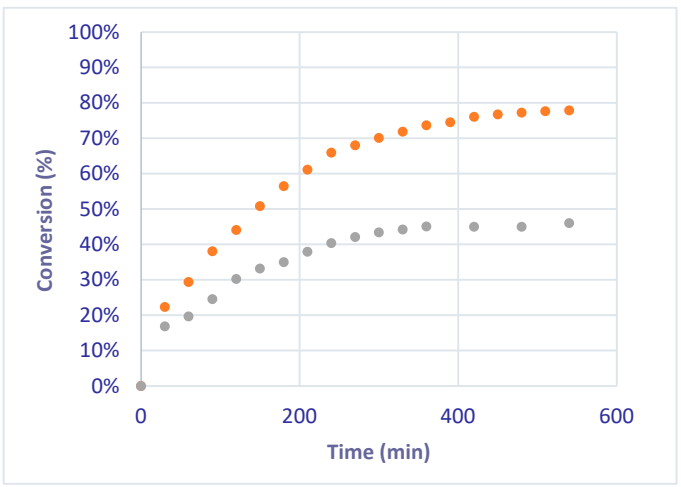

(**a**)

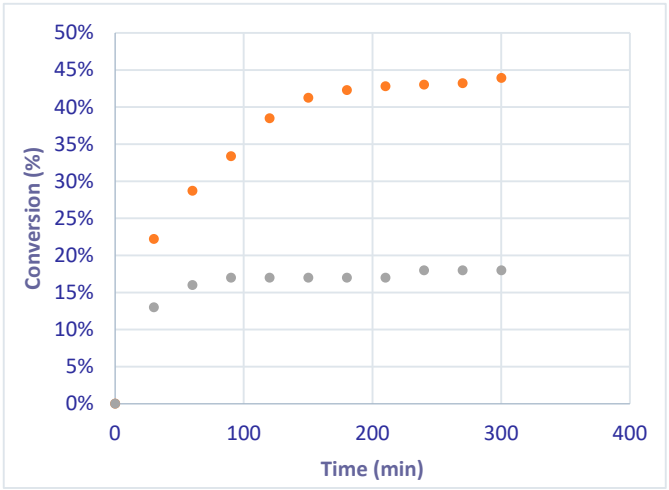

(**b**)

Figure 6. Conversion of phenylacetylene under FcFR and EcFR (1 Hz) modes at 2 mL/min (**a**) and 5 mL/min (**b**) flow rates. Orange dots: conversions measured under the EcFR mode. Grey dots: conversions measured under the FcFR mode.

4. Discussion

Under our conditions (conversion < 90% and high selectivity), the kinetic rate for the hydrogenation reaction can be approximated by the following expression [31] with respect to the liquid reagent (P_h) and the dissolved H_{2ls} at the catalyst surface.

$$r = \frac{wk_1[H_{2ls}][P_h]}{(1 + K_B[Ph])^2} = k[H_{2ls}] \quad (3)$$

According to [31], at 323 K, and as a first approximation, the values of k_1 and K_B are 0.00889 and 3.4, respectively. Considering the amount of Pd given by ICP-AES af-

ter the 120 h experiments (818 ± 24 mg/kg) and the packing foam volume, we obtain w = 0.045 kg/m^3 under our conditions. Finally, considering the liquid mass flow rate Q_l, the inlet phenylacetylene concentration (P_{h0} = 0.25 kmol/m^3), the liquid concentration of H_{2l} at saturation (calculated under a working temperature of 323 K and pressure of 1 atm: $[H_{2l}]^*$ = 323 kmol/m^3), and the kinetic rate given by Equation (1), it is easy to calculate the theoretical conversion (χ) under kinetic regime (i.e., $[H_{2ls}] = [H_{2l}]^*$), as follows:

$$\chi = \frac{rV}{Q_l P_{h0}} \quad (4)$$

Table 2 gives the theoretical (kinetic regime Equation (4)) and experimental conversions under our conditions for both the FcFR and EcFR (1 Hz) modes. It is important to note here that the kinetic rate considered in this work was not optimized for the Pd@PDA@PUF catalyst used in this work but, rather, for a Pd/C catalyst [31]. However, as to the best of our knowledge, no kinetic study for Pd@PDA is available in the open literature we used as a first approximation the kinetic rate developed by Chaudhari et al. [31].

Table 2. Kinetic conversion versus the FcFR/EcFR mode.

Liquid Flow	Theoretical Conversion (Equation (4))	Experimental Conversion—FcFR	Experimental Conversion—EcFR
2 mL/min	85.8%	44%	78%
5 mL/min	39.8%	19%	45%

We can see that for the EcFR mode, the experimental data are close to the theoretical values obtained from the kinetic regime [31]. In contrast to the FcFR mode (limited by gas–liquid mass transfer), the kinetic regime occurs with the EcFR mode. In other words, the EcFR is not limited by the mass transfer efficiency with the kinetic rate used in this work. This interesting result can be explained by the fact that the cycles in the EcFR mode generate more shear stress and consequently produce a lot of small bubbles compared to the FcFR mode (see Figure 7).

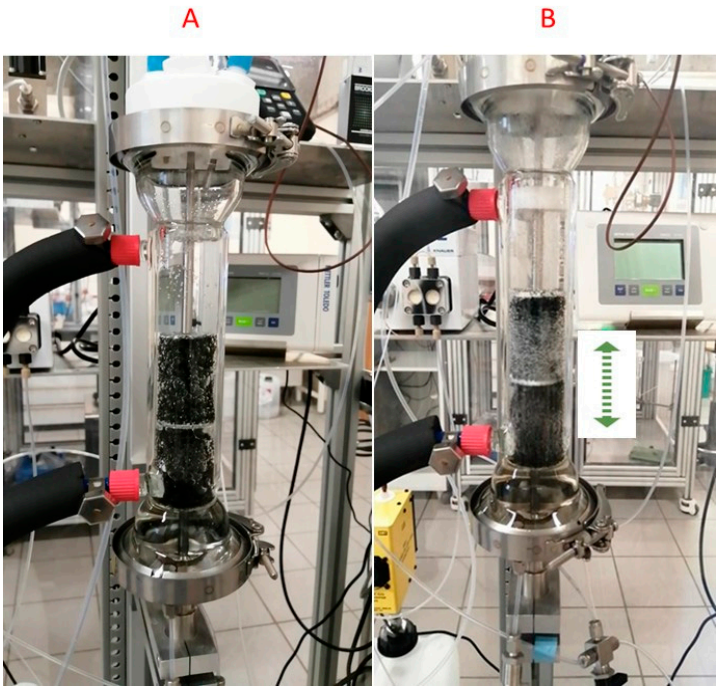

Figure 7. Image of gas bubbles in the column for both the FcFR (**A**) and EcFR (**B**) modes.

The modelling of this system (especially for the EcFR mode) is not straightforward because both the parameters and boundary conditions of the partial differential equation relevant for the mass balance are time-variant (see for instance [25]). The numerical solution is therefore difficult and corresponds to the well-known *Stefan problem*. However, since pure hydrogen (H_2) has been used in this work and the pressure drop remains negligible for both FcFR and EcFR, we can assume a simple mass transfer film model in order to compare, as a first approximation, the performance of the FcFR and EcFR modes. In this approach, the thickness of the liquid film is constant over the reactor length, the molecular diffusivity does not vary with the liquid composition, and the reactor operates in the isotherm mode. Under these conditions, the mass transfer analysis for multiphase reactions expresses the overall reaction rate, r, in terms of the saturated solubility of H_2 in the liquid near the catalytic surface, H_{2ls}, and a sum of the mass transfer resistances K_{ov} [32]. For the foam packing, this method has been successfully used to estimate mass transfer from catalytic chemical reactions [33,34].

$$K_{ov}([H_2^*] - [H_{2ls}])\varepsilon_l = r \tag{5}$$

where H_2^* is the liquid concentration of H_2 at saturation and ε_l the liquid fraction of the bed defined by $\varepsilon = \varepsilon_l + \varepsilon_g$.

The global mass transfer resistances consist of (i) gas absorption into the liquid ($k_{gl}a_l$), (ii) diffusion of the dissolved gas from the bulk liquid to the catalyst surface ($k_{ls}a_s$), and (iii) diffusion of the species inside the porous catalyst as represented by the effectiveness factor η. Correlations (or experimental procedures) have been already developed for estimating both $k_{gl}a_l$ and $k_{ls}a_s$ for a foam-bed reactor [11,34]. However, it is difficult to adapt these methods to our conditions. It is more accurate to lump the resistances into an overall mass transfer coefficient (k_{la}). Given that the thickness of the PDA layer is established to be less than 20 nm, the effectiveness factor η can be considered to be equal to 1 and we can assume that the reaction is limited only by mass transfer. Consequently, we consider the following expression:

$$\frac{1}{K_{ov}} = \left(\frac{1}{k_{gl}a_l} + \frac{1}{k_{ls}a_s} + \frac{1}{\eta k}\right) \approx \left(\frac{1}{k_{la}} + + \frac{1}{\eta k}\right) \approx \left(\frac{1}{k_{la}} + \frac{1}{k}\right) \tag{6}$$

From FcFR experimental data and Equations (4)–(6), the k_la values are estimated at 8.1×10^{-4} and 9.8×10^{-4} for 2 and 5 mL/min, respectively.

In the literature, k_{la} is usually correlated with the Reynolds and Schmidt numbers, which can be expressed as [25]

$$\frac{a_{GL}\varepsilon_L}{a_c} S_h = 0.026 R_{eL}^{0.5} S_c^{0.5} \tag{7}$$

As a first approximation, the k_{la} values found in this work (i.e., by a chemical catalytic reaction method) are of the same order as the values given by the correlation [25] obtained by a physical method, i.e., CO_2 dissolution, see Figure 8 and Table 3.

Table 3. k_{la} values estimated from the Kov method or calculated by the correlation [25].

	FcFR/FFR		EcFR/EFR	
Q_L (mL/min)	**This Work**	**With Correlation**	**This Work**	**With Correlation**
2	8.1×10^{-4}	9.1×10^{-4}	-	9.7×10^{-3}
5	9.8×10^{-4}	2.3×10^{-3}	-	1.5×10^{-2}

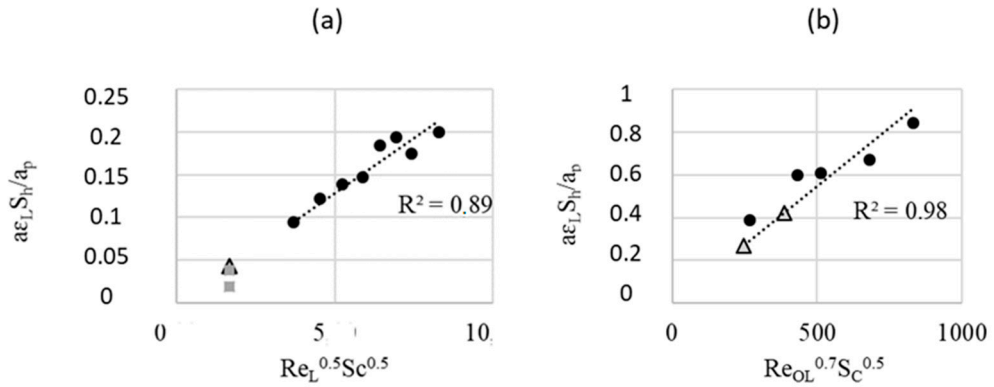

Figure 8. Sherwood number versus Re: spherical (experimental values of [25]), squares (this work), and triangles (values calculated from Equation (8)): FcFR mode (**a**) and EcFR (1 Hz) (**b**).

For the EcFR mode, since the chemical kinetic regime occurs, the *kla* values cannot be estimated from the experimental data. However, they can be calculated by the correlation proposed by Michaud et al. [25] obtained under non-catalytic conditions (i.e., for EFR) (Figure 8).

$$\frac{a_{GL}\overline{\varepsilon_L}}{a_c} S_h = 0.00109 R_{eOL}^{0.7} S_c^{0.5} \quad (8)$$

with the following Reynolds Oscillation number

$$Re_{oL} = \frac{U_{LO}\rho_L \varphi}{L} \text{ with } \begin{cases} U_{LO} = U_L + \left(\frac{2\pi f V_{Lo}}{S}\right) \\ V_{LO} = \varepsilon_{Li} L_o (1-\tau_i) S - \varepsilon_{Lmax} L_o (1-\tau_{max}) S \end{cases}$$

where f is the oscillation frequency (1 Hz), V_{LO} represents the liquid volume displaced by compression/relaxation of the foams at high frequencies, $\tau_{i/}\tau_{max}$ the initial or maximal compressed ratio (i.e., 40%/80%), and $\varepsilon_{Li}/\varepsilon_{Lmax}$ the initial and final liquid holdup.

The k_{la} values obtained from both the correlations and this work (i.e., by a chemical catalytic reaction method) are given in Table 3. It can be seen that the k_{la} values estimated in this work from chemical data are close to the values calculated from the correlation of Michaud et al. [25]. This result thus seems to confirm the kinetic model used by default in Equation (5).

5. Conclusions

The unambiguous results obtained in this work demonstrate, for the first time, the concept of the elastic catalytic foam bed reactor (EcFR). Thanks to the remarkable adhesive properties of polydopamine, no catalyst leaching is observed under continuous gas–liquid operation with a high frequency of compression/relaxation cycles.

The interesting performance achieved with this new technology breakthrough for multiphase reactors opens the way to new catalytic strategies for intensifying gas–liquid processes. In the low interaction regime (e.g., bubble regime), the performance of the 'conventional' fixed catalytic foam-bed reactor (FcFR) is close to the expected value in terms of gas–liquid mass transfer efficiency. In contrast, the liquid mixing conditions for the EcFR appear to be imposed by the foam compression/relaxation cycles, resulting in an insensitive effect of the liquid flow rate on the global mass transfer. For all the experimental data obtained in this work, the pressure drop due to the packing foam remains negligible for both FcFR and EcFR (i.e., close to 15 Pa/m). Consequently, only the energy consumed by the mini-motor to ensure the rotation of the crankshaft was considered. Notably, its maximum power capacity of 35 W was never reached under the experimental conditions tested in this study.

Greater enhancement would be possible at higher frequencies but, as it is often the case with the EFR reactor, thermodynamic equilibrium interferes with thorough analysis [25].

Under our conditions, we can say that the EcFR technology is a new way of intensifying the process by increasing mass transfer at constant energy.

Author Contributions: Conceptualization, D.E.; methodology, D.E. and M.M.; calculus, M.F. and D.E.; validation, D.E., M.M. and M.F.; formal analysis, M.M. and M.F.; investigation, H.P., M.M. and M.F.; resources, D.E. and V.R.; data curation, M.M. and M.F.; writing—original draft preparation, M.M. and D.E.; writing—review editing, D.E. and V.R.; visualization, M.F. and M.M.; supervision, D.E.; project administration, D.E.; funding acquisition, D.E. and V.R. All authors have read and agreed to the published version of the manuscript.

Funding: This research was funded by the Agence National de la Recherche (project 'EFR'), grant number ANR-22-CE51-0007 (D.E.), and the University of Strasbourg (IdEX Unistra 2019) (V.R.). H.P. thanks the international doctoral program of the Université de Strasbourg for his PhD fellowship.

Data Availability Statement: The original contributions presented in the study are included in the article, further inquiries can be directed to the corresponding author.

Acknowledgments: Thierry Romero (ICPEES, UMR 7515) is gratefully acknowledged for acquiring the HR-SEM images. Eliott Edouard (CP2M, UMR 5128) is thanked for his help in the Pd@PDA@PUF preparation samples.

Conflicts of Interest: The authors declare no conflicts of interest.

Nomenclature

a	Window (or pore) diameter, μm
a_{GL}	Interfacial gas–liquid area per unit volume of liquid, $m^2{}_L\ m^{-3}{}_L$
a_p	Packing surface area per unit volume, $m^2 \cdot m^{-3}$
a_c	Specific surface area ($m^2 \cdot m^{-3}$)
C	Concentration $mol \cdot m^{-3}$
D_{ax}	Axial dispersion coefficient in the liquid phase, $m^2 \cdot s^{-1}$
D_R	Reactor diameter, mm
d_s	Struts diameter, m
H_e	Henry coefficient, $m^3 L$ Pa mol^{-1}
ID	Internal diameter of the cylindric foam blocs, mm
k_1	Kinetic constant, (m^6/kmol·kg·s)
K_B	Kinetic constant, m^3/kmol
K	Rate constant, s^{-1}
k_{la}	Overall gas–liquid mass transfer coefficient, s^{-1}
L_0	length of an initial block foam, m
L	Reactor length, m
Q_L	Liquid flowrate, mL/min
Q_G	Gas flowrate, NmL/min
R	Universal gas constant, 8314 $Pa \cdot m^3\ K^{-1}\ mol^{-1}$
Re_L	Modified Reynolds number for the liquid phase, dimensionless
Re_{OL}	Modified Oscillation Reynolds for the liquid phase, dimensionless
r	Hydrogenation rate of phenylacetylene $kmol \cdot L^{-1} \cdot s^{-1}$
S	Selectivity
Sc	Schmidt number, dimensionless
Sh	Sherwood number, dimensionless
t	Time, s
tc	Residence time, s^{-1}
T	Temperature, K
u_g	Superficial gas phase velocity, $m \cdot s^{-1}$
u_l *(or Ul)*	Superficial liquid phase velocity, $m \cdot s^{-1}$
V	Reactor volume, m^3
w	Mass of catalyst (Pd) by reactor volume, kg/m^3
X	Conversion, dimensionless

Greek symbols:

E	Foam porosity, dimensionless
ε_l	Liquid holdup, dimensionless
ε_g	Gas holdup, dimensionless
ϕ	Cell diameter, μm
$\tau_{1,2,(t)}$	Compression ratio, dimensionless

Abbreviations:

EcFR	Elastic Catalytic Foam-bed Reactor
EFR	Elastic Foam-bed Reactor
FcFR	Fixed Catalytic Foam-bed Reactor
GC	Gas chromatography
ICP-AES	Inductively coupled plasma atomic emission spectroscopy
PDA	Polydopamine
PUF	Polyurethane foam

References

1. Langley, N.; Harrison, S.; Van Hille, R. A critical evaluation of CO_2 supplementation to algal systems by direct injection. *Biochem. Eng. J.* **2012**, *68*, 70–75. [CrossRef]
2. Utikar, R.P.; Ranade, V. Intensifying multiphase reactions and reactors strategies and examples. *ACS Sustain. Chem. Eng.* **2017**, *5*, 3607–3622. [CrossRef]
3. Mills, P.L.; Duduković, M.P. Analysis of catalyst effectiveness in trickle-bed reactors processing volatile or nonvolatile reactants. *Chem. Eng. Sci.* **1980**, *35*, 2267–2279. [CrossRef]
4. Baharudin, L.; Inder, A.; Watson, M.; Yip, A. Process intensification in multifunctional reactors: A review of multi-functionlity by catalytic structures, internals, operating modes, and unit integrations. *Chem. Eng. Process.* **2021**, *168*, 108561. [CrossRef]
5. Nigam, K.D.P.; Larachi, F. Process intensification in trickle-bed reactors. *Chem. Eng. Sci.* **2005**, *60*, 5880–5894. [CrossRef]
6. Lacroix, M.; Nguyen, P.; Schweich, D.; Pham-Huu, C.; Poncet, S.S.; Edouard, D. Pressure drop measurements and modeling on SiC foams. *Chem. Eng. Sci.* **2007**, *62*, 3259–3267. [CrossRef]
7. Edouard, D.; Lacroix, M.; Pham, C.; Mbodji, M.; Pham-Huu, C. Experimental measurements and multiphase flow models in solid SiC foam beds. *AIChE* **2008**, *54*, 2823–2832. [CrossRef]
8. Stemmet, C.P.; Jongmans, J.N.; van der Schaaf, J.; Kuster, B.F.M.; Schouten, J.C. Hydrodynamics of gas–liquid counter-current flow in solid foam packings. *Chem. Eng. Sci.* **2005**, *60*, 6422–6429. [CrossRef]
9. Stemmet, C.P.; Van der Schaaf, J.; Kuster, B.F.M.; Schouten, J.C. Solid foam packings for multiphase reactors. Modelling of liquid holdup and mass transfer. *Chem. Eng. Res. Des.* **2006**, *84*, 1134–1141. [CrossRef]
10. Stemmet, C.P.; Meeuwse, M.; van der Schaaf, J.; Kuster, B.F.M.; Schouten, J.C. Gas–liquid mass transfer and axial dispersion in solid foam packings. *Chem. Eng. Sci.* **2007**, *62*, 5444–5450. [CrossRef]
11. Saber, M.; Huu, T.T.; Pham-Huu, C.; Edouard, D. Residence time distribution, axial liquid dispersion and dynamic–static liquid mass transfer in trickle flow reactor containing β-SiC open-cell foams. *Chem. Eng. J.* **2012**, *185–186*, 294–299. [CrossRef]
12. Zapico, R.R.; Marín, P.; Díez, F.V.; Ordóñez, S. Liquid hold-up and gas–liquid mass transfer in an alumina open-cell foam. *Chem. Eng. Sci.* **2016**, *143*, 297–304. [CrossRef]
13. Nguyen, T.; Swesi, Y.; Edouard, D.; Fongarland, P. Platelet Millireactor Filled with Open Cell Foam-Supported Pt Nanoparticles for a Three-Phase Catalytic System. *Ind. Eng. Chem. Res.* **2019**, *58*, 9352–9361. [CrossRef]
14. Cai, X.; Wörner, M.; Marschall, H.; Deutschmann, O. Numerical study on the wettability depend interaction of a rising bubble with a periodic open cell cellular structure. *Catal. Today.* **2016**, *273*, 151–160. [CrossRef]
15. Lämmermann, M.; Horak, G.; Schwieger, W.; Freund, H. Periodic open cellular structures (POCS) for intensification of multiphase ractors: Liquid holdup and two-phase presure drop. *Chem. Eng. Process.* **2018**, *126*, 178–189. [CrossRef]
16. Lange, R.; Hanika, J.; Stradiotto, D.; Hudgins, R.R.; Silveston, P.L. Investigations of periodically operated trickle-bed reactors. *Chem. Eng. Sci.* **1994**, *49*, 5615–5621. [CrossRef]
17. Castellari, A.T.; Haure, P.M. Experimental study of the periodic operation of a trickle-bed reactor. *AIChE* **1995**, *41*, 1593–1597. [CrossRef]
18. Banchero, M.; Manna, L.; Sicardi, S.; Ferri, A. Experimental investigation of fast mode liquid modulation in a trickle-bed reactor. *Chem. Eng. Sci.* **2004**, *59*, 4149–4154. [CrossRef]
19. Boelhouwer, J.G.; Piepers, H.W.; Drinkenburg, B.A.H. Advantages of forced non-steady operated trickle-Bed reactors. *Chem. Eng. Technol.* **2002**, *25*, 647–650. [CrossRef]
20. Dietrich, W.; Grünewald, M.; Agar, D.W. Dynamic modelling of periodically wetted catalyst particles. *Chem. Eng. Sci.* **2005**, *60*, 6254–6261. [CrossRef]
21. Härting, H.U.; Lange, R.; Larachi, F.; Schubert, M. A novel inclined rotating tubular fixed bed reactor concept for enhancement of reaction rates and adjustment of flow regimes. *Chem. Eng. J.* **2015**, *281*, 931–944. [CrossRef]
22. Dashliborun, A.M.; Larachi, F.; Taghavi, S.M. Gas-liquid mass-transfer behavior of packed-bed scrubbers for floating/offshore CO_2 capture. *Chem. Eng. J.* **2019**, *377*, 119236. [CrossRef]

23. Ferroni, C.; Bracconi, M.; Ambrosetti, M.; Groppi, G.; Maestri, M.; Freund, H.; Tronconi, E. Process intensification in mass-transfer limited catalytic reactors through anisotropic periodic open cellular structures. *Chem. Eng. Process.* **2024**, *195*, 109613. [CrossRef]
24. Duduković, M.P.; Larachi, F.; Mills, P.L. Multiphase catalytic reactors: A perspective on current knowledge and future trends. *Catal. Rev.* **2002**, *44*, 123–246. [CrossRef]
25. Michaud, M.; Bornette, F.; Rautu, E.; More, S.H.; Martinez Mendez, M.L.; Jierry, L.; Edouard, D. Unprecented continuous elastic foam-bed reactor for CO_2 capture. *Chem. Eng. J.* **2023**, *452*, 138604. [CrossRef]
26. Lefebvre, L.; Kelber, J.; Jierry, L.; Ritleng, V.; Edouard, D. Polydopamine-coated open cell polyurethane foam as an efficient and easy-to-regenerate soft structured catalytic support (S_2CS) for the reduction of dye. *J. Environ. Chem. Eng.* **2017**, *5*, 79–85. [CrossRef]
27. Pardieu, E.; Chau, N.T.T.; Dintzer, T.; Romero, T.; Favier, D.; Roland, T.; Edouard, D.; Jierry, L.; Ritleng, V. Polydopamine-coated open cell polyurethane foams as an inexpensive, flexible yet robust catalyst support: A proof of concept. *Chem. Commun.* **2016**, *52*, 4691–4693. [CrossRef] [PubMed]
28. Ait Khouya, A.; Mendez Martinez, M.L.; Bertani, P.; Romero, T.; Favier, D.; Roland, T.; Guidal, V.; Bellière-Baca, V.; Edouard, D.; Jierry, L.; et al. Coating of polydopamine on polyurethane open cell foams to design soft structured supports for molecular catalysts. *Chem. Commun.* **2019**, *55*, 11960–11963. [CrossRef]
29. Simfoam. Available online: https://simfoam.alsace.cnrs.fr/Web/Home.aspx (accessed on 10 April 2024).
30. Peng, H.; Zhang, X.; Papaefthimiou, V.; Pham-Huu, C.; Ritleng, V. Pd-functionalized polydopamine-coated polyurethane foam: A readily prepared and highly reusable structured catalyst for selective alkyne semi-hydrogenation and Suzuki coupling under air. *Green Chem.* **2023**, *25*, 264–279. [CrossRef]
31. Chaudhari, R.V.; Jaganathan, R.; Kolhe, D.S.; Emig, G.; Hofmann, H. Kinetic modelling of a complex consecutive reaction in a slurry reactor: Hydrogenation of phenylacetylene. *Chem. Eng. Sci.* **1986**, *41*, 3073–3081. [CrossRef]
32. Ramachandran, P.A.; Chaudhari, R.V. *Three-Phase Catalytic Reactors*; Gordon and Breach; Science Publishers: New York, NY, USA, 1983.
33. Lévêque, J.; Philippe, R.; Zanota, M.; Meille, V.; Sarrazin, F.; Baussaron, L.; De Bellefon, C. Hydrodynamics and mass transfer in a tubular reactor containing foam packings for intensification of G-L-S catalytic reactions in co-current up-flow configuration. *Chem. Eng. Res. Design* **2016**, *109*, 686–697. [CrossRef]
34. Bouras, H.; Haroun, Y.; Philippe, R.; Augier, F.; Fongarland, P. CFD modeling of mass transfer in gas-liquid-solid catalytic reactors. *Chem. Eng. Sci.* **2021**, *233*, 116378. [CrossRef]